

# Higher-order QED corrections to single- $W$ production in electron–positron collisions

G. Montagna<sup>1</sup>, M. Moretti<sup>2</sup>, O. Nicrosini<sup>3</sup>, A. Pallavicini<sup>1</sup>, F. Piccinini<sup>3</sup>

<sup>1</sup> Dipartimento di Fisica Nucleare e Teorica, Università di Pavia and INFN, Sezione di Pavia, via A. Bassi 6, 27100 Pavia, Italy

<sup>2</sup> Dipartimento di Fisica, Università di Ferrara and INFN, Sezione di Ferrara, Ferrara, Italy

<sup>3</sup> INFN, Sezione di Pavia and Dipartimento di Fisica Nucleare e Teorica, Università di Pavia, via A. Bassi 6, 27100 Pavia, Italy

Received: 5 October 2000 /

Published online: 11 May 2001 – © Springer-Verlag / Società Italiana di Fisica 2001

**Abstract.** Four-fermion processes with a particle lost in the beam pipe are studied at LEP to perform precision tests of the electroweak theory. Leading higher-order QED corrections to such processes are analyzed within the framework of the structure function (SF) approach. The energy scale entering the QED SF is determined by inspection of the soft and collinear limit of the  $O(\alpha)$  radiative corrections to the four-fermion final states, paying particular attention to the process of single- $W$  production. Numerical predictions are shown in realistic situations for LEP experiments and compared with existing results. A Monte Carlo event generator, including exact tree-level matrix elements, vacuum polarization, higher-order leading QED corrections and anomalous trilinear gauge couplings, is presented.

## 1 Introduction

Four-fermion final states are of special interest for the physics program of LEP2 and future high-energy electron–positron colliders, being entangled with electroweak gauge boson production and decay [1]. In particular, the process considered in the present paper, i.e.,

$$e^+e^- \rightarrow e^-(e^+)\bar{\nu}_e(\nu_e)q'\bar{q}, \quad (1)$$

is peculiar among all the possible four-fermion final states because the bulk of its cross section is due to two sub-processes, i.e.,  $W$ -boson pair production and decay,

$$e^+e^- \rightarrow W^*W^* \rightarrow 4 \text{ fermions}, \quad (2)$$

and the radiation of an almost on-shell  $t$ -channel photon from the electron (positron), with subsequent production of a  $W$ -boson and a neutrino,

$$e^+e^- \rightarrow \gamma^*e^+(e^-) \rightarrow W^*\bar{\nu}_e(e^-) \rightarrow 4 \text{ fermions}. \quad (3)$$

Despite that, strictly speaking, the two sub-processes (2) and (3) always occur simultaneously and are indistinguishable, channel (2) dominates if the electron is emitted at a large angle, whereas channel (3) dominates if the electron is emitted in the very forward region, because of the presence of a quasi-real  $t$ -channel photon.

In this paper the process (3) will be addressed, by restricting the analysis to the kinematical range of forwardly emitted electrons. This signal is usually referred to as single- $W$  production, since only the two final jets are detected [2].

The importance of this process has been emphasized since a long time. In the LEP2 energy range it is fundamental in order to study the self-interaction of the gauge bosons, together with the process (2), whereas in the energy regime of future colliders at the TeV scale it becomes the dominant electroweak process. In [3,4] cross sections and distributions were calculated in the approximation of real  $W$ -boson production, either by [3] studying the reaction  $e^+e^- \rightarrow e^-\bar{\nu}_eW^+$ , or by [4,5] employing the Weizsäcker–Williams [6] equivalent-photon approximation for the  $t$ -channel photon. In [3–5] was pointed out the relevance of this process for the study of trilinear gauge boson couplings and some assessment of the sensitivity has been given. The first full four-fermion calculation, including the crucial effect of the fermion masses, has been presented in [7], where the LEP2 sensitivity to anomalous gauge couplings has been studied. Since then, other complete four-fermion calculations of the single- $W$  process have appeared in the literature and implemented in computational tools for data analysis [7–11]. In most of these calculations the effect of the fermion masses is exactly accounted for in the dynamics and kinematics for the whole four-fermion phase space [7,8,10,11], while in the approach of [9] the Weizsäcker–Williams approximation is employed in the very forward, collinear region and matched with a massless four-fermion computation outside it. An up-to-date inventory of the present theoretical status is under preparation by the four-fermion working group of the LEP2 MC workshop at CERN [12].

Measurements of the single- $W$  cross section and the corresponding bounds on anomalous gauge couplings have

been recently reported by the LEP collaborations [2]. Because the foreseen accuracy of the final LEP2 data is of the order of 1%–2% [12], accurate theoretical predictions for the cross section and distributions are required.

The calculation of the cross section for single- $W$  processes poses several non-trivial theoretical problems [12]. For a realistic account of the gauge boson properties it is mandatory to include the gauge boson width in the propagator. In general, this mixes a fixed order calculation with an all order resummation of a class of Feynman diagrams and introduces a violation of the Ward identities of the theory. This issue is of special importance here since, due to the  $t$ -channel photon exchange, even a tiny violation of the QED Ward identities is enhanced by a factor of  $s/m_e^2$ . This is indeed the case if a running width is used in the calculation. This problem has been extensively studied [13–15], and several options to address it have been explored. The theoretically most appealing procedure is the fermion loop scheme [14, 15], which preserves both  $U(1)$  and  $SU(2)$  Ward identities. Recently, this scheme has been generalized to the case of massive external fermions, both in its minimal version, which considers the imaginary parts of the fermionic loops (IFL) [8], and in its full realization with real and imaginary parts [16, 17]. In particular, in [8] a detailed numerical investigation has been performed, showing no significant difference between the IFL and the fixed width scheme, even in the region most sensible to  $U(1)$  gauge invariance. For this reason, the fixed width scheme is adopted in the present calculation.

Another delicate issue is the so called resolved-photon component of the cross section. The quasi-real  $t$ -channel photon can split into a pair of almost massless quarks, leading to a situation where the partonic picture of hadrons is inadequate and both perturbative and non-perturbative QCD corrections become relevant. This issue is widely discussed in the literature [18], where the standard approach to this problem is also described and to which the reader is referred for details. However, for single- $W$ -like events the resolved-photon component does not constitute a severe limitation: once a hard  $q\bar{q}$  invariant mass cut is imposed, as done in realistic data analysis, the bulk of the signal is kept, whereas the resolved photon contribution becomes almost negligible [9].

A further relevant issue is given by radiative corrections due to photon radiation. Given the particular kinematical configuration of the single- $W$  process with a charged particle lost in the beam pipe, the question naturally arises whether a leading log (LL) description is meaningful. Actually, by looking at the tree-level differential distribution of the virtual photon four-momentum transfer  $t$ , the largest part of the events are characterized by a ratio  $t/m_e^2 \gg 1$ , so that a LL approximation is viable. Because exact  $O(\alpha)$  electroweak corrections to single- $W$  production are still unknown, in most of the theoretical and experimental studies presented so far, only the large contribution of initial-state radiation (ISR) has been taken into account, generally by using the collinear structure function (hereafter denoted as SF) and assuming  $s = 4E^2$  as the proper scale for QED radiation. Due

to the dominance of the quasi-real  $t$ -channel photon exchange, this can be expected not to be a suitable choice in the present case. On the other hand, it has recently been proposed to correct only the  $s$ -channel contributions to the single- $W$  signature, fixing the radiation scale in the usual manner, and to neglect the photonic corrections to the  $t$ -channel contributions [10]. Following previous investigations [19–23] of the pattern of photonic radiation in QED and electroweak processes, some theoretical arguments to determine the appropriate energy scale entering the SF are presented and compared with existing results. The analysis here described elucidates the theoretical details and provides further numerical results of the contribution by the authors of [24] to the activity of the four-fermion working group of the LEP2 MC workshop at CERN [12]. Ideas similar to those adopted in the present work have recently appeared in [25] and there have been applied to the two-photon process  $e^+e^- \rightarrow e^+e^-\mu^+\mu^-$ .

This paper is organized as follows. After a short review of the SF approach to LL QED corrections in Sect. 2, Sect. 3 collects the analytical results valid for soft and collinear corrections to a generic scattering process. By comparing the results of Sect. 2 and Sect. 3, the radiation scales for single- $W$  production are determined in Sect. 4. Section 5 deals with the problem of taking into account the effect of the photon vacuum polarization in the single- $W$  process, while Sect. 6 shows the numerical results of the present study obtained with a Monte Carlo (hereafter MC) code for the single- $W$  signature, including also the effect of anomalous trilinear gauge couplings. Conclusions and prospects are given in Sect. 7.

## 2 Structure function approach to photon radiation

Since in high-energy processes the corrections due to the emission of soft and collinear radiation are quite large, the LL contribution must be calculated at every perturbative order. A common technique to achieve this goal is the QED structure function approach [26], which consists in convoluting the hard-scattering cross section with appropriate “parton” densities. As is well known, these convolution factors, i.e., the QED structure functions, include, by construction, both the real and virtual part of the photon correction, in order to ensure the cancellation of the infrared singularities. If a generic Born-level prediction  $d\sigma_0$  is considered, the cross section  $d\sigma$  including LL QED radiative corrections is obtained, by virtue of factorization theorems, according to the following general formula [26]:

$$d\sigma = \prod_i \int dx_i D(A^2, x_i) d\sigma_0, \quad (4)$$

where  $1 - x_i$  are the energy fractions carried away by the radiated photons from the  $i$ th leg,  $A$  is the characteristic scale of the SF  $D(A^2, x_i)$ , whose evolution is

driven by the Dokshitzer–Gribov–Lipatov–Altarelli–Paris (DGLAP) equation [27] and is dependent on  $\Lambda$ . It is worth noticing that the choice of the scale  $\Lambda$  is not dictated by general arguments; it is therefore rather arbitrary.

Equation (4) can be rewritten by stressing the possibility of different scales for each SF as follows:

$$d\sigma = \prod_i \int dx_i D(\Lambda_i^2, x_i) d\sigma_0. \quad (5)$$

In particular, if the integrated hard-scattering cross section is a smooth function of the centre of mass (c.m.) energy, once the integrations over the energy fractions  $x_i$  are performed in the soft-photon approximation, the  $O(\alpha)$  double-log expansion of (5) can be written as follows:

$$d\sigma = d\sigma_0 \left( 1 + \sum_i \frac{\alpha}{\pi} \log \frac{\Delta E}{E} L(\Lambda_i^2) \right), \quad (6)$$

where  $\Delta E/E$  is the maximum energy for undetected photons, to be identified with finite energy resolution of the photon detector, and  $L(\Lambda_i^2) \equiv \log(\Lambda_i^2/m^2)$  is the collinear logarithm.

Since the functional form of the QED SF is accurately known [26], the main problem in evaluating (5) is to fix the process scales  $\Lambda_i$ . A generally adopted attitude is given by the comparison of (6) with a perturbative calculation, which can be performed within any approximation, provided it reproduces the correct double-log contribution of the  $O(\alpha)$  correction. This issue is addressed in the next section.

### 3 Analytical results

The double-log contribution to photon radiation traces back to soft and collinear bremsstrahlung and its virtual counterpart [28], and, in the case of a calorimetric measurement of the energy of the final-state (FS) particles, to hard radiation collinear to the FS particles themselves [29–32]. At each perturbative order, the leading contribution can be expanded in terms of infrared and collinear logs. For example, when the photons are emitted from the initial-state (IS) particles only, such an expansion can be arranged in terms of double-log contributions of the form  $\alpha^n l^n L_s^n$ , where  $l \equiv \log(\Delta E/E)$  is the infrared log and  $L_s \equiv \log(s/m^2)$  is the collinear log. This is the reason why  $\Lambda^2 = s$  is the “natural” energy scale to be used for SF in the presence of ISR only. When also FS radiation is considered, the collinear log,  $L$ , is in general modified by additional factors coming from the angular integration over the photon variables. A typical example is given by the radiation emitted from one leg in the  $t$ -channel QED contribution to Bhabha scattering [19]. In the soft-photon approximation the radiation cones, one from the IS electron and one from the FS electron, have a half-opening which is determined by the angle between the emitting particles, because of a destructive interference. As a consequence, the energy scale  $s$ , which appears

in  $L_s$ , transforms into  $|t| \simeq s(1 - \cos\theta)$ , where  $\theta$  is the electron scattering angle, and, therefore,  $L_s \rightarrow L_t$ . Hence, the perturbative expansion contains collinear logs which are modified because of the angular ordering introduced by the radiation cones. In the presence of large scattering angles, for which  $|t| \simeq s$ , the above modification is numerically small, but it becomes more and more important in the forward angular range, which is the dynamically favorite region by  $t$ -channel Bhabha scattering and where  $t \ll s$ . The net result is a numerically significant depletion of QED radiation effects just in the most important part of the hard-scattering  $t$ -channel dynamics. Actually, when using SF to evaluate QED LL corrections to small-angle Bhabha scattering, the energy scale  $\Lambda^2 = |t|$  is employed in all phenomenological applications [19]. More in general, in order to take into account dominant initial–final-state interference effects in addition to initial- and final-state leading terms,  $s$  and  $t$  QED contributions to Bhabha scattering can be corrected for in terms of a unique combination of Mandelstam invariants given by  $st/u$ , as discussed in [20, 21]. Therefore, the energy scale  $\Lambda^2 = st/u$  turns out to be a suitable choice for the evaluation in terms of SF of LL corrections to QED Bhabha scattering, as demonstrated, in comparison with the exact  $O(\alpha)$  calculation, in [21]. Similar arguments for an appropriate choice of the energy scale for QED radiation, based on the inspection of the soft and collinear limit of the  $O(\alpha)$  correction, have also been advocated in [22] for the reaction  $e^+e^- \rightarrow W^+W^-$  and, very recently, in [25] for the process  $e^+e^- \rightarrow e^+e^-\mu^+\mu^-$ . Comparisons performed in [22, 25] with available exact  $O(\alpha)$  calculations explicitly exhibit the validity of such a strategy, which is therefore pursued in the present analysis. As already remarked, the result for LL corrections in the presence of a calorimetric detection of FS particles must include the contribution of photons which, regardless of their energy, cannot be discriminated from closely collinear fermions, as a consequence of the finite angular resolution of the calorimeters. The role of such hard photons collinear to the FS particles becomes, therefore, unavoidable in the case of a calorimetric measurement of the energy of the FS particles, as discussed in the following.

#### 3.1 Soft-photon contribution

In this section the contribution of photons too soft to be detected in the calorimeter will be computed for a generic process with  $n$  ingoing legs<sup>1</sup>. The following approximations are understood:

$$\begin{cases} q_i \gg k, \\ s_{ij} \gg m_i^2, m_j^2, \end{cases} \quad (7)$$

where  $q_i$  is the momentum of a particle of mass  $m_i$  emitting a real photon of momentum  $k$ , and  $s_{ij} \equiv (q_i + q_j)^2$  is the invariant mass of the pair  $ij$ .

<sup>1</sup> This choice fixes our conventions. Outgoing particles will appear as ingoing ones with momentum and charge according to crossing symmetry

By following the standard derivation of the eikonal factors due to soft bremsstrahlung and by generalizing it to particles with different masses and charges, the differential cross section, dressed by soft-photon emission, can be cast into the following factorized form [28]:

$$d\sigma_{\text{soft}} = d\sigma_0 \frac{d\omega}{\omega} \frac{2\alpha}{\pi} \sum_{i>j}^n Q_i Q_j \log \frac{s_{ij}}{m_i m_j}, \quad (8)$$

where  $\omega$  is the photon energy and  $Q_i$  is the charge of the  $i$ th particle.

It is worth noticing that in the limit  $s_{ij} \ll m_i^2, m_j^2$ , provided the first inequality in (7) still holds, the logarithmic behavior present in (8) disappears, leaving a power law which can be simply obtained by means of the substitution [28]

$$\log \frac{s_{ij}}{m_i m_j} \longrightarrow \frac{1}{3} \frac{s_{ij}}{m_i m_j}. \quad (9)$$

Notice that, since the goal is to determine the scale entering the SF, only the contribution of real photons is explicitly calculated, because the virtual corrections, in order to preserve the cancellations of infrared singularities, must share the same leading collinear structure of the real part itself.

By including the virtual part needed to cancel the infrared singularity and integrating (8) over the photon energy  $\omega$  in the soft region  $0 \leq \omega \leq \Delta E$ , one gets

$$d\sigma_{\text{S+V}} = d\sigma_0 \log \frac{\Delta E}{E} \frac{2\alpha}{\pi} \sum_{i>j}^n Q_i Q_j \log \frac{s_{ij}}{m_i m_j}. \quad (10)$$

### 3.2 Hard radiation collinear to the final-state particles

In the case of a calorimetric set-up, which is the realistic situation for single- $W$  production at LEP, photons collinear to the detected FS particles cannot be distinguished from the emitting particles themselves, independently of the photon energy. Therefore, in order to obtain the correct structure of double-log corrections for such an event selection, the effect due to the emission of unresolved hard radiation collinear to the FS particles must be taken into account in addition to soft + virtual corrections.

To this end, let us reconsider the previous process with  $n$  ingoing legs and pretend  $m$  of them to be changed into outgoing legs at the end of the calculation (see the previous footnote). Then, the contribution of photons collinear to the FS particles can be cast into a gauge invariant form as follows [30–32]:

$$d\sigma_{\text{hard}} = d\sigma_0 \frac{d\omega}{\omega} \frac{2\alpha}{\pi} \sum_i^m Q_i^2 \log \frac{E_i \delta}{m_i}, \quad (11)$$

where  $E_i$  is the energy of the  $i$ th particle, and  $\delta$  is the half-opening angle of the calorimetric resolution.

By integrating (11) over the photon energy  $\omega$  in the range  $\Delta E \leq \omega \leq E$ , the integrated correction due to hard

photons collinear to the FS particles is given by

$$d\sigma_{\text{hard}} = d\sigma_0 \log \frac{E}{\Delta E} \frac{2\alpha}{\pi} \sum_i^m Q_i^2 \log \frac{E_i \delta}{m_i}. \quad (12)$$

### 3.3 The master formula

Equations (10) and (12) give the leading double-log contribution which must be compared to (6), the  $O(\alpha)$  perturbative expansion of (5), in order to fix the process scales  $\Lambda_i$ . Summing the contributions of (10) and (12), the analytical cross section is in conclusion given by

$$\begin{aligned} & d\sigma_{\text{S+V}} + d\sigma_{\text{hard}} \\ &= d\sigma_0 \frac{2\alpha}{\pi} \log \frac{\Delta E}{E} \left\{ \sum_{i=m+1}^n Q_i^2 \log \frac{E_i}{m_i} \right. \\ & \quad \left. - \sum_{i>j}^n Q_i Q_j \log 2(1 - c_{ij}) - \sum_i^m Q_i^2 \log \delta \right\}, \quad (13) \end{aligned}$$

where  $c_{ij}$  is the cosine of the angle between particles  $i$  and  $j$ .

Three different kinds of logarithms occur in (13). The first term contains the mass and energy logarithms of the IS particles only, since, as expected, the energies and the masses of the FS particles disappeared, in agreement with the KLN theorem [33]. The second term includes angular terms due to radiation interference, while the third one comes from the requirement of calorimetric measurement.

These terms must be compared with the collinear logarithms of (6) in order to fix the scales  $\Lambda_i$  of the SF. In the following section this task is accomplished in detail for the single- $W$  process.

## 4 Fixing the radiation scales in the single- $W$ process

Let us consider, for definiteness, the process  $e^+e^- \rightarrow e^- \bar{\nu} u \bar{d}$  with the FS electron lost in the beam pipe (single- $W$  process). In this event selection (hereafter ES) the leading contribution comes from  $\gamma^*e^+$  scattering with the virtual photon emitted from the electron line. The leading dynamics is given by the  $t$ -channel Feynman diagrams shown in Fig. 1.

If a calorimetric measurement of the energies of the FS particles is performed, only the IS legs need to be corrected by the SF. Furthermore, since the electron is scattered in the very forward region, the interference between the electron line and the rest of the process is very small. This allows for a natural sharing of the logarithms coming from (13) between the two IS SF associated to the colliding electron and positron.

Hence the formula (13), when compared with (6), translates into the two following scales ( $\Lambda_-$  refers to SF attached to the electron line, while  $\Lambda_+$  refers to the SF

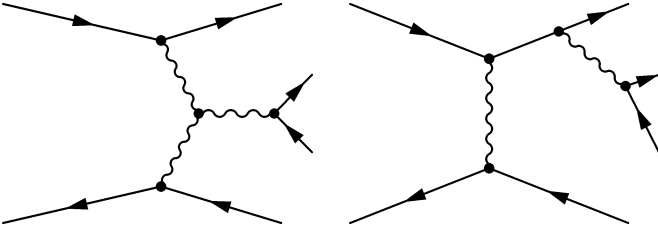


**Fig. 1.** The fusion and bremsstrahlung diagrams are the leading Feynman graphs for the single- $W$  signature

attached to the positron line),

$$\begin{aligned} A_-^2 &= 4E^2 \frac{(1 - c_-)^2}{\delta^2}, \\ A_+^2 &= 2^{14/9} E^2 \frac{((1 - c_{\bar{d}})(1 - c_u)^2)^{2/3}}{((1 - c_{u\bar{d}})^2 \delta^5)^{2/9}}, \end{aligned} \quad (14)$$

where  $E$  is the beam energy,  $c_-$  is the cosine of the electron scattering angle,  $c_u$  and  $c_{\bar{d}}$  are the cosine of the quark scattering angles with respect to the initial positron, and  $c_{u\bar{d}}$  is the cosine of the relative angle between the quarks.

It is worth noticing that in the numerical implementation, whenever one of the two scales is less than a small cutoff ( $A_{\text{cutoff}}^2 = 4m_e^2$ , where  $m_e$  is the electron mass), the radiation from the corresponding leg is switched off, in accordance with (9). It was carefully tested that variations of the cutoff do not alter the numerical results.

Owing to the presence of a resonant  $W$ -boson, some modifications to the previous results may come from finite-width effects and from radiation decoherence [34]. Finite-width corrections of the form of  $E_\gamma/\Gamma_W$  arise when the unstable particle propagator goes off its mass shell, but this is not the present case, since the multi-fermion final state can accommodate a resonant  $W$ . Radiation decoherence is present whenever a resonance occurs and its effect is to cancel the angular dependence from the scale. As a consequence the scale  $A_+$  should be modified by dropping the angular interference factors in (14) when the emitted photons have  $E_\gamma \sim \Gamma_W$ . Yet in the present case the effect is tiny, since the effects due to angular interference for the scale  $A_+$  are already small by themselves.

It is also possible to make a naive ansatz for the radiation scales without a detailed calculation, by thinking of the graphs of Fig. 1 in terms of the Weizsäcker–Williams approximation [6], i.e., in terms of a convolution of the process  $e^+\gamma \rightarrow \nu_e W^*$  with an equivalent-photon spectrum plus a real electron line. This leads to assigning two different scales to the single- $W$  process: one scale for the electron current and one for the positron current. The former scale is the proper one for a  $t$ -channel process, e.g.  $t$ -channel Bhabha scattering, so it is simply  $|q_{\gamma^*}^2|$ , where  $|q_{\gamma^*}^2|$  is the squared momentum transfer in the  $ee\gamma^*$  vertex. The latter is the sum of an  $s$ -channel electron exchange and a  $t$ -channel  $W$  exchange (see Fig. 1). Assuming that the  $t$ -channel dominates, its natural cutoff is given by the  $W$ -boson mass,  $M_W$ . Hence, the following ansatz follows:

$$A_{-, \text{naive}}^2 = |q_{\gamma^*}^2|, \quad A_{+, \text{naive}}^2 = M_W^2, \quad (15)$$

where  $M_W$  is the mass of the  $W$ -boson. The comparison between the scales given by (14) and these naive scales, which will be performed numerically in the following section, provides a useful cross-check of the analytical results derived by inspection with the soft/collinear limit of the  $O(\alpha)$  correction.

A discussion of other possible approaches to the treatment of photonic corrections to single- $W$  production can be found in the four-fermion working group report of the LEP2 MC Workshop [12].

## 5 The running of the electromagnetic coupling constant

Besides the higher-order QED corrections discussed in the previous sections, other large logarithmic contributions to the single- $W$  cross section arise from the running of the electromagnetic coupling constant  $\alpha$ . Since in the case under study the dominant configurations come from the Feynman diagrams with an almost on-shell photon exchange, the appropriate scale for the evaluation of the electromagnetic coupling relative to the  $t$ -channel photon in the  $ee\gamma^*$  vertex is the squared momentum transfer  $q_{\gamma^*}^2$  defined above.

However, because  $G_F$ ,  $M_W$  and  $M_Z$  are the typically adopted input parameters for electroweak processes at LEP2, the electromagnetic coupling is fixed at tree level to a high energy value as, for example,

$$\alpha_{G_F} = 4\sqrt{2} \frac{G_F M_W^2 s_W^2}{4\pi}, \quad \text{with} \quad s_W^2 = 1 - \frac{M_W^2}{M_Z^2}. \quad (16)$$

On the other hand, the single- $W$  production is a  $q_{\gamma^*}^2 \simeq 0$  dominated process and therefore the above high-energy evaluation of  $\alpha$ ,  $\alpha_{G_F}$ , needs to be rescaled to its correct value at small momentum transfer. To this end, a gauge-invariant “reweighting” procedure can be adopted, by rescaling the differential cross section  $d\sigma/dt$  ( $t \equiv q_{\gamma^*}^2$ ) in the following way:

$$\frac{d\sigma}{dt} \rightarrow \frac{\alpha^2(t)}{\alpha_{G_F}^2} \frac{d\sigma}{dt}, \quad (17)$$

where  $\alpha(t)$  is the running coupling constant computed at virtuality  $q_{\gamma^*}^2$ .

A detailed analysis of the effect of the running couplings in single- $W$  production has recently been performed within the massive fermion loop scheme in [17], where the couplings are automatically running in the calculation. As shown in [17], the relative difference between the above reweighting prescription and the complete results of the fermion loop scheme is at the 1%–2% level<sup>2</sup>, and it is therefore in the expected range of the theoretical uncertainty due to missing full one-loop electroweak corrections.

<sup>2</sup> Actually, for the single- $W$  final state under examination here and for realistic event selections, the differences between the two procedures are confined below the 1% level

**Table 1.** The ES adopted for the calculations shown in the present paper for the signature  $e^+e^- \rightarrow e^-\bar{\nu}_e u \bar{d}$ , according to [12]

electron angular acceptance	$ \cos\theta_e  > 0.997$	$ \cos\theta_e  > 0.997$
quarks angular acceptance	1. no cut	2. $ \cos\theta_{q,\bar{q}}  < 0.95$
calorimetric half-opening angle	$5.00^\circ$	$5.00^\circ$
quark-antiquark invariant mass	45.0 GeV	45.0 GeV

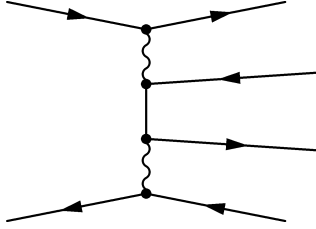


**Fig. 2.** The multiperipheral diagram is the main sub-leading Feynman graph for the single- $W$  signature

## 6 Numerical results

In this section the MC code, developed to simulate the single- $W$  process, is described and a sample of numerical results obtained by means of it is shown and commented on, with particular emphasis on the effects of higher-order QED corrections to single- $W$  production at LEP2 energies.

### 6.1 The Monte Carlo code

A MC program, named SWAP, was developed to calculate cross sections and differential distributions for the single- $W$  signature.

As already emphasized, the main feature of this process is the fact that the  $t$ -channel photon of Fig. 1 becomes quasi-real. In the limit of massless fermions, the photon propagator becomes singular in the forward direction and the cross section develops a logarithmic singularity. Indeed, whenever the final electron is lost in the beam pipe, its mass becomes a natural cutoff for the very forward singularities, compelling one to build a massive matrix element and phase space. The phase-space integration is performed in SWAP with the aid of a multi-channel importance sampling with stratification. The main peaking structures for the single- $W$  process are given by the dynamics depicted by the fusion and bremsstrahlung graphs of Fig. 1. They are the resonant  $W$ -boson invariant mass, treated with a Breit–Wigner weight, and the  $t$ -channel “singularity” of the quasi-real photon, treated with a  $1/|t|$  weight. Moreover, the program can deal with the singularities of the sub-leading  $t$ -channel CC20 diagrams shown in Fig. 2, by means of the multi-channel approach.

The exact hard-scattering matrix element is computed by means of the ALPHA code [35] for the automatic evaluation of Born scattering amplitudes. Fermion masses are exactly taken into account and the fixed width scheme is

adopted as gauge-restoring approach, by taking the massive gauge boson propagator as follows:

$$\Pi^{\mu\nu} = \frac{-i \left( g^{\mu\nu} - \frac{k^\mu k^\nu}{M^2 - i\Gamma M} \right)}{k^2 - M^2 + i\Gamma M}, \quad \Gamma = \text{const.} \quad (18)$$

It is known [8,14,15] that this scheme preserves  $U(1)$  gauge invariance but still violates  $SU(2)$  Ward identities. However, at least in the unitary gauge employed here, it is indistinguishable from other fully gauge-invariant schemes [8,14,15].

The contribution of anomalous gauge couplings is also accounted for in SWAP. The anomalous gauge boson couplings  $\Delta k_\gamma$ ,  $\lambda_\gamma$ ,  $\delta_Z$ ,  $\Delta k_Z$  and  $\lambda_\gamma$  are implemented in the ALPHA code according to the parameterization of [38,39]. Photon radiation is implemented via the SF formalism, according to the discussion of Sect. 4. It is worth noticing that, since the incoming electron/positron are required to be on-shell massive fermions, a naive four-momentum rescaling, due to photon emission, such as  $\hat{p}_\pm = xp_\pm$  leads to potentially dangerous gauge violations, according to our previous discussion. Therefore, the rescaled incoming four-momenta are implemented as

$$\hat{p}_\pm = (xE, 0, 0, \pm\sqrt{x^2E^2 - m_e^2}),$$

by interpreting  $x$  as the energy fraction after photon radiation, as motivated in [21]. If required,  $p_\perp/p_L$  effects can be provided in the treatment of ISR, by means of either  $p_\perp$ -dependent SF [36] or a QED parton shower algorithm [21,37]. The effect of vacuum polarization is taken into account as described by (17), by including the contribution of leptons, heavy quarks and light quarks, the latter according to the parameterization of [40]. The program supports realistic ES and it can be employed either as a cross section calculator or as an event generator, with both weighted and unweighted generation available.

The technical precision of the event generator SWAP has already been carefully proved in [12], by means of detailed tuned comparisons between the predictions of independent codes. Perfect agreement was found, both at the level of integrated cross sections and distributions, also for purely leptonic final states.

### 6.2 Discussion of the numerical results

The numerical simulations are elaborated according to the ES reviewed in Table 1, with the electroweak input parameters shown in Table 2.

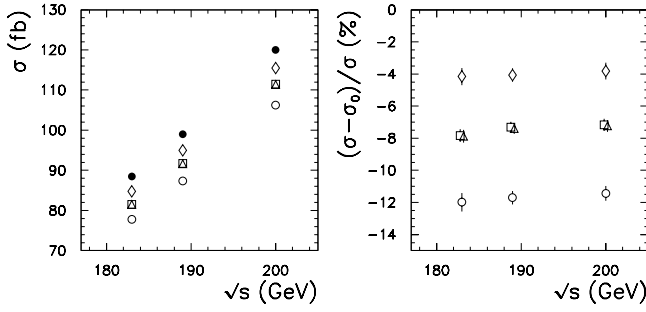


**Fig. 3.** The effects of LL QED corrections to the cross section of the single- $W$  process  $e^+e^- \rightarrow e^-\bar{\nu}u\bar{d}$  for different choices of the energy scale in the electron/positron SF. The quark angular acceptance  $0^\circ \leq \vartheta_{u,\bar{d}} \leq 180^\circ$  is considered. Left: absolute cross values as functions of the LEP2 c.m. energy. Right: relative difference between the QED corrected cross sections and the Born one, still as functions of the c.m. energy. The marker  $\bullet$  represents the Born cross section,  $\circ$  represents the correction given by  $\Lambda_\pm^2 = s$  for both SF,  $\diamond$  the correction given by the scales  $\Lambda_\pm^2 = |q_{\gamma^*}^2|$  for both SF,  $\square$  the correction given by the naive scales of (15),  $\triangle$  the correction given by the scales of (14). The entries correspond to  $s^{1/2} = 183, 189, 200$  GeV. The markers are misplaced for better reading

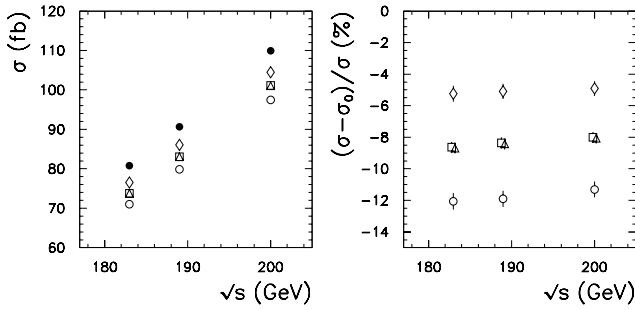


**Fig. 4.** The same as Fig. 3 for the quark angular acceptance  $|\cos \theta_{u,\bar{d}}| < 0.95$

**Table 2.** The adopted electroweak input parameters, according to [12]. All other parameters are calculated by means of the tree-level relations

$G_F = 1.16637 \times 10^{-5} \text{ GeV}^{-2}$
$M_Z = 91.1867 \text{ GeV}$
$M_W = 80.35 \text{ GeV}$
$\Gamma_Z = 2.49471 \text{ GeV}$

In Figs. 3 and 4 the numerical impact of different choices of the  $\Lambda^2$ -scale on the cross section of the single- $W$  process  $e^+e^- \rightarrow e^-\bar{\nu}u\bar{d}$  in the LEP2 energy range is shown. Since the energy scale  $\Lambda_+$  of (14) depends on the quark scattering angles, two different quark angular acceptances are considered, namely no cut (Fig. 3) and  $|\cos \vartheta_{u,\bar{d}}| < 0.95$  (Fig. 4). The marker  $\bullet$  represents the Born cross section,  $\circ$  represents the correction given by the  $\Lambda_\pm^2 = s$  scale for both IS SF,  $\diamond$  represents the correction given by the  $\Lambda_\pm^2 = |q_{\gamma^*}^2|$  scale for both IS SF,  $\triangle$  the correction given by the scales of (14),  $\square$  the correction

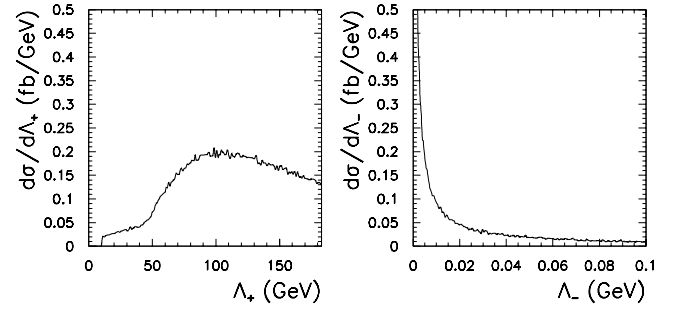


**Fig. 5.** The differential cross sections of the single- $W$  process  $e^+e^- \rightarrow e^-\bar{\nu}u\bar{d}$  with respect to the two scales of (14) at  $s^{1/2} = 189$  GeV

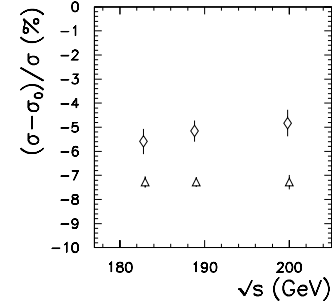


**Fig. 6.** The effects of the rescaling of  $\alpha_{\text{QED}}$  from  $\alpha_{G_F}$  to  $\alpha(q_{\gamma^*}^2 = 0)$  ( $\triangle$ ) and  $\alpha(q_{\gamma^*}^2)$  ( $\diamond$ ) on the integrated cross section of the single- $W$  process  $e^+e^- \rightarrow e^-\bar{\nu}u\bar{d}$ .  $\sigma_0$  is the cross section computed in terms of  $\alpha_{G_F}$ . The entries correspond to  $s^{1/2} = 183, 189, 200$  GeV

given by the naive scales of (15). It can be seen that neither the  $s$  scale, as implemented in some computational tools used for the analysis of the single- $W$  process, nor the  $|q_{\gamma^*}^2|$  scale are able to reproduce the effects due to the scales of (14) and (15). These two scales are in good agreement and both predict a lowering of the Born cross section of about 8%–9%, almost independent of the c.m. LEP2 energy and quark angular acceptance. This fact can be understood by looking at Fig. 5, where the single- $W$  differential cross section is shown with respect to the scales  $\Lambda_\pm$  of (14). On the left,  $\Lambda_+$  exhibits a broad peak not far from  $M_W$ , while, on the right, the other scale  $\Lambda_-$  peaks, as expected, at very small momentum transfer.

Figure 6 shows the effects of the reweighting procedure of (17) for the evaluation of the QED running coupling constant. The marker  $\triangle$  represents the relative difference between the integrated cross section computed in terms of  $\alpha_{G_F}$  and the cross section computed in terms of  $\alpha(0)$ , while the marker  $\diamond$  is the relative difference between the integrated cross section computed in terms of  $\alpha_{G_F}$  and the cross section computed in terms of  $\alpha(t)$ . As can be seen, the rescaling from  $\alpha_{G_F}$  to  $\alpha(t)$  introduces a negative correction of about 5%–6% in the LEP2 energy range. The difference between  $\triangle$  and  $\diamond$ , which is about 2%–3%, is a measure of the running of  $\alpha_{\text{QED}}$  from  $q_{\gamma^*}^2 = 0$  to  $q_{\gamma^*}^2 = t$ .

As an illustrative example of the effect of anomalous couplings on single- $W$  differential distributions, in Fig. 7 the distribution of the  $q\bar{q}$  invariant mass, around the peak

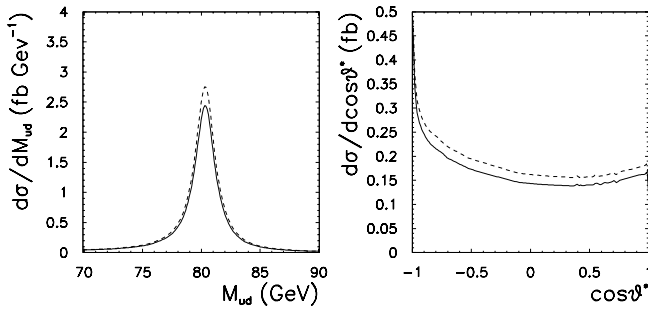


**Fig. 7.** The single- $W$  differential cross sections with respect to the quark–antiquark invariant mass (left side), and with respect to the angle between a quark and the line of flight of the reconstructed  $W$ -boson in the frame of rest of the  $W$ -boson (right side). The dashed line represents the distribution in the presence of an anomalous gauge coupling  $\Delta\kappa_\gamma = 0.1$ , while the solid line is the standard model prediction. The c.m. energy is  $s^{1/2} = 189$  GeV

of the  $W$ -boson resonance, and the distribution of the angle of the quarks with the line of flight of the reconstructed  $W$ -boson in the  $W$ -boson rest frame are shown. The dashed lines correspond to the simulation as obtained by means of SWAP for the anomalous coupling  $\Delta\kappa_\gamma = 0.1$ , while the solid lines represent the standard model prediction. The effect of the anomalous coupling  $\Delta\kappa_\gamma$  at LEP2 energies is just an overall rescaling of the total cross section. Therefore, the LEP2 sensitivity to  $\Delta\kappa_\gamma$  in single- $W$  events depends crucially on the accuracy of the theoretical evaluation of the total cross section.

## 7 Conclusions

The process of single- $W$  production in high-energy  $e^+e^-$  collisions is relevant at LEP2 for the determination of the non-abelian self-couplings of the  $W$ -boson, and of primary importance at future Linear Colliders at the TeV scale, its cross section being dominant at very high energies with respect to other four-fermion processes.

In order to give a contribution to the reduction of the theoretical uncertainty presently associated to the calculation of the single- $W$  cross section, the issue of higher-order photonic corrections has been carefully investigated within the standard SF technique. Theoretical and phenomenological arguments for the choice of the energy scale entering the SF have been proposed. Two possible solutions for the scale of QED radiation have been obtained. The former has been derived by means of general arguments concerning the soft and collinear limit of the  $O(\alpha)$  corrections coming from the radiation of external legs. The latter, which can be considered as a naive ansatz, has been driven by thinking of the single- $W$  process in terms of the Weizsäcker–Williams approximation.

Numerical calculations show that the typically adopted choice of the center of mass energy of the reaction, as radiation scale for the process, can lead to an overestimate of the radiative correction by a factor of 1.5, implying an underestimate of the cross section of about

4%. Also the choice of fixing the scale to the momentum transfer  $t$  in the  $ee\gamma^*$  vertex for both the IS SF leads to an underestimate of the photon correction of about 4%. The difference between the predictions given by the two set of scales of (14) and (15) is at the per mille level in the LEP2 energy range. Therefore, the naive scales of (15) provide a good ansatz for the energy scale of QED radiation in the single- $W$  process, which could be simply implemented in MC tools for data analysis and further corroborated by comparison with the results of other approaches. The method here described for the energy scale determination in the SF can be simply generalized to other four-fermion process dominated by non-annihilation channels, such as single- $Z$  production.

In order to provide adequate phenomenological predictions for precision experiments, also the running of the electromagnetic coupling constant has been accounted for in an effective way, i.e., by rescaling the differential cross section for the ratio of the electromagnetic coupling constant, evaluated at the typical scale of the process, to the same coupling evaluated from the input parameters according to tree-level relations. The effect of such rescaling amounts to a negative correction of about 5%–6%, in agreement with recent findings [17], as far as the effect of  $\alpha_{\text{QED}}$  is concerned.

In the light of the experimental precision for the single- $W$  process, the corrections considered in the present paper are phenomenologically relevant.

According to the theoretical approach described in the present paper, an original MC program SWAP has been developed, including exact tree-level matrix elements with finite fermion masses effects, anomalous couplings, vacuum polarization and higher-order QED corrections. The code is available for experimental analysis.

*Acknowledgements.* The authors wish to thank the members of the four-fermion working group of the LEP2 Monte Carlo Workshop (CERN), in particular Y. Kurihara, G. Passarino, R. Pittau and M. Verzocchi, for useful discussions on the subject. A. Pallavicini is grateful to the INFN, Sezione di Pavia, for having provided computer facilities.

## References

1. Physics at LEP2, edited by G. Altarelli, T. Sjöstrand, F. Zwirner (CERN 96-01, Geneva, 1996); G. Montagna, O. Nicrosini, F. Piccinini, Riv. Nuovo Cim. **21**, 1 (1998), hep-ph/9802302, and references therein
2. ALEPH Coll., R. Barate et al., Phys. Lett. B **462**, 389 (1999); L3 Coll., M. Acciarri et al., Phys. Lett. B **436**, 417 (1998); DELPHI Coll., P. Abreu et al., Phys. Lett. B **423**, 194 (1998); R. Tanaka, hep-ex/9811039, Proceedings of the 29th International Conference on High-Energy Physics (ICHEP98), Vancouver, Canada, 23–29 July 1998
3. J. Ellis, M.K. Gaillard, CERN Report 76-18, 21 (1976); A. Donnachie, K.J.F. Gaemers, Z. Phys. C **4**, 37 (1980); K. Neufeld, Z. Phys. C **17**, 145 (1983)
4. E. Gabrielli, Mod. Phys. Lett. A **1**, 465 (1986)
5. U. Baur, B.A. Kniehl, J.A.M. Vermaseren, D. Zeppenfeld, Proceedings of Large Hadron Collider Workshop (CERN



- 90-10, Geneva, 1990) Vol. II, p. 956; U. Baur, J.A.M. Vermaseren, D. Zeppenfeld, Nucl. Phys. B **375**, 3 (1992); E.N. Argyres, C.G. Papadopoulos, Phys. Lett. B **263**, 298 (1991)
6. C.F. Weizsäcker, Z. Phys. **88**, 612 (1934); E.J. Williams, Phys. Rev. **45**, 729 (1934); see also S. Frixione, M. Mangano, P. Nason, G. Ridolfi, Phys. Lett. B **319**, 339 (1993)
7. T. Tsukamoto, Y. Kurihara, Phys. Lett. B **389**, 162 (1996)
8. E. Accomando, A. Ballestrero, E. Maina, Phys. Lett. B **479**, 209 (2000)
9. G. Passarino, The single- $W$  production case, hep-ph/9810416
10. E.E. Boos, M.N. Dubinin, Single- $W$  production at Linear Colliders, hep-ph/9909214
11. F.A. Berends, C.G. Papadopoulos, R. Pittau, Four-fermion production in electron-positron collisions with NEXTCALIBUR, hep-ph/0002249
12. M. Grünewald, G. Passarino et al., Report of the four-fermion working group of the LEP2 MC workshop (CERN), in preparation; see also <http://www.to.infn.it/~giampier/lep2.html>
13. Y. Kurihara, D. Perret-Gallix, Y. Shimizu, Phys. Lett. B **349**, 367 (1995); U. Baur, D. Zeppenfeld, Phys. Rev. Lett. **75**, 1002 (1995)
14. E.N. Argyres et al., Phys. Lett. B **358**, 339 (1995)
15. W. Beenakker et al. Nucl. Phys. B **500**, 255 (1997)
16. G. Passarino, Unstable particles and non-conserved currents: a generalization of the fermion loop scheme, hep-ph/9911482
17. G. Passarino, Single- $W$  production and fermion loop scheme: numerical results, hep-ph/0001212
18. G.A. Schuler, T. Sjöstrand, Z. Phys. C **73**, 677 (1997) and references therein; P. Aurenche, G.A. Schuler et al., in Physics at LEP2, edited by G. Altarelli, T. Sjöstrand, F. Zwirner (CERN 96-01, Geneva, 1996), Vol. 1, p. 291, hep-ph/9601317 and references therein
19. See, for example, G. Montagna, O. Nicrosini, F. Piccinini, Phys. Lett. B **358**, 348 (1996); S. Jadach, M. Melles, B.F.L. Ward, S.A. Yost, Acta Phys. Polon. B **30**, 1745 (1999)
20. M. Greco, O. Nicrosini, Phys. Lett. B **240**, 219 (1990)
21. C.M. Carloni Calame, C. Lunardini, G. Montagna, O. Nicrosini, F. Piccinini, Large-angle Bhabha scattering and luminosity at flavour factories, hep-ph/0003268
22. W. Beenakker, F.A. Berends et al., in Physics at LEP2, edited by G. Altarelli, T. Sjöstrand, F. Zwirner (CERN 96-01, Geneva, 1996), Vol. 1, p. 79, hep-ph/9602351; W. Beenakker, A. Denner, Standard model predictions for  $W$ -pair production in electron-positron collisions, DESY 94-051
23. W. Beenakker, F.A. Berends, W.L. van Neerven, Proceedings of Radiative Corrections for  $e^+e^-$  collisions, edited by J.H. Kühn (Springer-Verlag, 1989), p. 3
24. G. Montagna et al., On photon radiation in single- $W$  process, talk given by A. Pallavicini at the meeting of the LEP2 MC workshop, CERN, 12/10/1999, see <http://www.to.infn.it/~giampier/lep2.html>
25. Y. Kurihara et al., QED radiative corrections to the non-annihilation processes using the structure function and the parton shower, hep-ph/9912520
26. E.A. Kuraev, V. Fadin, Sov. J. Nucl. Phys. **41**, 466 (1985); G. Altarelli, G. Martinelli, in Physics at LEP, edited by J. Ellis, R. Peccei (CERN 86-02, Geneva, 1986), Vol. 1 p. 47; O. Nicrosini, L. Trentadue, Phys. Lett. B **196**, 551 (1987); Z. Phys. C **39**, 479 (1998); F.A. Berends, G. Burgers, W.L. van Neerven, Nucl. Phys. B **297**, 429 (1988); S. Jadach, M. Skrzypek, Z. Phys. C **49**, 577 (1991); M. Skrzypek, Acta Phys. Pol. B **23**, 135 (1992); M. Cacciari, A. Deandrea, G. Montagna, O. Nicrosini Europhys. Lett. **17**, 123 (1992); G. Montagna, O. Nicrosini, F. Piccinini, Phys. Lett. B **406**, 243 (1997); A.B. Arbuzov, Phys. Lett. B **470**, 252 (1999)
27. V.N. Gribov, L.N. Lipatov, Sov. J. Nucl. Phys. **15**, 298 (1972); G. Altarelli, G. Parisi, Nucl. Phys. B **126**, 298 (1977); Y.L. Dokshitzer, Sov. Phys. JETP **46**, 641 (1977)
28. See, for example, D.R. Yennie, S.C. Frautschi, H. Suura, Ann. Phys. **13**, 379 (1961); G. Pancheri, Phys. Lett. B **315**, 477 (1993)
29. G. Sterman, S. Weinberg, Phys. Rev. Lett. **39**, 1436 (1977)
30. M. Caffo, R. Gatto, E. Remiddi, Nucl. Phys. B **252**, 378 (1985); Phys. Lett. B **139**, 439 (1984)
31. J. Fleischer, F. Jegerlehner, Z. Phys. C **26**, 629 (1985)
32. M. Cacciari, G. Montagna, O. Nicrosini, Phys. Lett. B **274**, 473 (1992)
33. F. Block, A. Nordsieck, Phys. Rev. **52**, 54 (1937); T. Kinoshita, J. Math. Phys. **3**, 650 (1962); T.D. Lee, M. Nauenberg, Phys. Rev. B **133**, 1549 (1964)
34. M. Greco, Riv. Nuovo Cim. **11**, 1 (1988)
35. F. Caravaglios, M. Moretti, Phys. Lett. B **358**, 332 (1995)
36. G. Montagna, M. Moretti, O. Nicrosini, F. Piccinini, Nucl. Phys. B **541**, 31 (1999); G. Montagna, O. Nicrosini, F. Piccinini, Comp. Phys. Commun. **98**, 206 (1996)
37. J. Fujimoto, T. Muehisa, Y. Shimizu, Prog. Theor. Phys. **90**, 177 (1993); Y. Kurihara, J. Fujimoto, T. Muehisa, Y. Shimizu, Prog. Theor. Phys. **95**, 375 (1996)
38. K. Gaemers, G. Gounaris, Z. Phys. C **1**, 259 (1979)
39. K. Hagiwara, K. Hikasa, R.D. Peccei, D. Zeppenfeld, Nucl. Phys. B **282**, 253 (1987)
40. S. Eidelman, F. Jegerlehner, Z. Phys. C **67**, 585 (1995)